



Cite this: *React. Chem. Eng.*, 2025, 10, 1216

Received 14th March 2025,  
 Accepted 22nd April 2025

DOI: 10.1039/d5re00119f

[rsc.li/reaction-engineering](https://rsc.li/reaction-engineering)

## Photocatalytic evolution of nitrous oxide from nitric monoxide over Pt-loaded titanium dioxide under UV irradiation†

Ryo Asayama,<sup>‡a</sup> Masanori Takemoto,<sup>‡a</sup> Arata Suzuki,<sup>a</sup> Ryuichi Watanabe,<sup>a</sup> Fuminao Kishimoto,<sup>‡a</sup> Kenta Iyoki,<sup>‡abc</sup> Tatsuya Okubo,<sup>‡a</sup> and Toru Wakihara<sup>‡ad</sup>

**This study presents a photocatalytic evolution of nitrous oxide (N<sub>2</sub>O) from nitric monoxide (NO), well known as a harmful gas contained in exhaust gas. Pt nanoparticles (NPs) were loaded on titanium dioxide (TiO<sub>2</sub>) using different methods including impregnation, photo-deposition and chemical reduction methods. Bare TiO<sub>2</sub> (without metal loading) did not exhibit high N<sub>2</sub>O evolution under UV irradiation, but all Pt-loaded TiO<sub>2</sub> photocatalysts did exhibit improved N<sub>2</sub>O evolution.**

Despite nitrous oxide (N<sub>2</sub>O) being the “third” greenhouse gas, it has recently attracted attention in various fields. In the petrochemical industry, selective oxidation of hydrocarbons is vital for producing valuable fine chemicals,<sup>1</sup> and there has been growing interest in utilizing green and atom-efficient oxidants such as H<sub>2</sub>O<sub>2</sub> and N<sub>2</sub>O for catalytic oxidation.<sup>2</sup> Both H<sub>2</sub>O<sub>2</sub> and N<sub>2</sub>O release monoatomic oxygen, forming harmless H<sub>2</sub>O and N<sub>2</sub>, respectively. N<sub>2</sub>O, in particular, is suitable as an oxidant in liquid and gas-phase reactions due to its high solubility in nonpolar media and gaseous nature. For instance, catalytic oxidation of CH<sub>4</sub> into methanol using N<sub>2</sub>O over zeolites has been proposed, converting two greenhouse gases into a useful chemical.<sup>3,4</sup> In the medical field, the demand of N<sub>2</sub>O, also known as “laughing gas,” has been increasing.<sup>5,6</sup> Considering these advantages, N<sub>2</sub>O holds significant potential for clean technologies in fine chemical synthesis and medical developments.

Plant-scale manufacturing of N<sub>2</sub>O was done at Jinhong Gas and Heng'an Gas Co., Ltd., where the decomposition of NH<sub>4</sub>-

NO<sub>3</sub> is used for N<sub>2</sub>O production. According to interviews with these companies, N<sub>2</sub>O produced through the current process is available to only high-end users in practical applications because of the high cost of the process (approximately 3000–5000 \$ per Mg).<sup>7</sup> The oxidation of NH<sub>3</sub> is considered an alternative reaction for N<sub>2</sub>O production.<sup>7,8</sup> However, there are concerns about the current price increase of NH<sub>3</sub>, which is probably a barrier to achieving inexpensive N<sub>2</sub>O production. As is well known, anthropogenic N<sub>2</sub>O is mainly released into the atmosphere during agricultural and industrial activities,<sup>9</sup> and N<sub>2</sub>O capture can be a promising technique for the effective utilization of N<sub>2</sub>O.<sup>10,11</sup> However, the concentration of N<sub>2</sub>O in the atmosphere is quite low (approximately 0.3–0.4 ppm). Many types of gas molecules, such as CO<sub>2</sub> and H<sub>2</sub>O, are also present in the atmosphere, which makes selective separation of N<sub>2</sub>O in the atmosphere further challenging. Considering the future demand of N<sub>2</sub>O, further implementation of low-cost N<sub>2</sub>O production is highly recommended.

Nitric monoxide (NO) is a well-known gaseous pollutant that mainly comes from the exhaust gases of automobiles, plants, and thermal power stations. In current de-NO<sub>x</sub> systems, NO is converted into N<sub>2</sub> through selective catalytic reduction with NH<sub>3</sub> over zeolites<sup>12,13</sup> or V-based TiO<sub>2</sub>.<sup>14,15</sup> before being discharged into the atmosphere. Recently, the use of NO as a feed gas for valuable nitrogen compounds has been a focus of research. For example, in several studies, the catalytic conversion of NO to NH<sub>3</sub> has been investigated.<sup>16–20</sup> Thus, NO has great potential as a feed gas toward the low-cost production of N<sub>2</sub>O.

Here, the photocatalytic evolution of N<sub>2</sub>O from NO as the feed gas over Pt-loaded TiO<sub>2</sub> is reported. Pt NPs were loaded onto TiO<sub>2</sub> (P25) using different loading methods. The photocatalysts hardly converted NO into N<sub>2</sub>O without ultraviolet (UV) irradiation, and the amount of N<sub>2</sub>O evolved increased under UV irradiation. Additionally, the Pt-loaded TiO<sub>2</sub> photocatalyst exhibited higher N<sub>2</sub>O evolution than did the bare TiO<sub>2</sub> photocatalyst, suggesting that Pt species can act as active sites in this case. These findings should help

<sup>a</sup> Department of Chemical System Engineering, The University of Tokyo, 7-3-1 Hongo, Bunkyo-ku, Tokyo 113-8656, Japan. E-mail: wakihara@chemsys.t.u-tokyo.ac.jp

<sup>b</sup> Precursory Research for Embryonic Science and Technology (PRESTO), Japan Science and Technology Agency (JST), Kawaguchi, Saitama 332-0012, Japan

<sup>c</sup> Department of Environment Systems, The University of Tokyo, 5-1-5 Kashiwanoha, Kashiwa-shi, Chiba 277-8563, Japan

<sup>d</sup> Institute of Engineering Innovation, The University of Tokyo, 2-11-16 Yayoi, Bunkyo-ku, Tokyo 113-8656, Japan

† Electronic supplementary information (ESI) available. See DOI: <https://doi.org/10.1039/d5re00119f>

‡ These authors contributed equally.



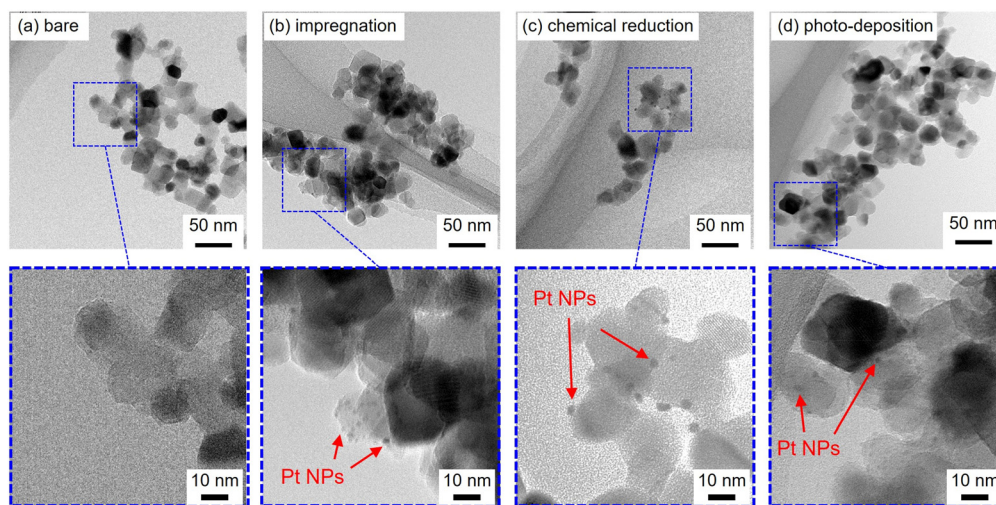


Fig. 1 TEM images of (a) bare and (b–d) Pt-loaded  $\text{TiO}_2$  photocatalysts prepared using different loading methods, namely (b) impregnation, (c) chemical reduction and (d) photo-deposition.

promote the development of  $\text{N}_2\text{O}$  production from a low-cost feedstock.

Pt-loaded  $\text{TiO}_2$  photocatalysts were synthesized using different loading methods, including chemical reduction, impregnation, and photo-deposition methods, and are denoted as Pt/ $\text{TiO}_2$ -cr, Pt/ $\text{TiO}_2$ -imp and Pt/ $\text{TiO}_2$ -pd, respectively. The details of the syntheses and characterizations of the photocatalysts are described in the ESI† Fig. 1 shows transmission electron microscopy (TEM) images of the bare and Pt-loaded  $\text{TiO}_2$  photocatalysts. Bare P25 was composed of small  $\text{TiO}_2$  NPs with diameters of less than 20 nm, as shown in Fig. 1(a). Spherical Pt NPs were located on the surface of the  $\text{TiO}_2$  NPs, and the Pt particles were less than 10 nm in diameter, as shown in Fig. 1(b–d). X-ray diffraction confirmed that the crystalline phase and the crystalline sizes of  $\text{TiO}_2$  were not affected by Pt loading (Fig. S1, Table S1†). All of the Pt-loaded  $\text{TiO}_2$  samples became black in color upon being loaded with Pt,

and UV-vis spectra of the Pt-loaded  $\text{TiO}_2$  indicated light absorption in the visible-light region, due to the surface plasmon resonance of Pt NPs (Fig. S2†). The characteristics of the Pt NPs in the Pt-loaded  $\text{TiO}_2$  photocatalysts are summarized in Table S1†. TEM images indicated that the particle sizes of Pt followed in the order Pt/ $\text{TiO}_2$ -cr > Pt/ $\text{TiO}_2$ -pd > Pt/ $\text{TiO}_2$ -imp. Dispersion of Pt determined from CO pulse measurements followed in the order Pt/ $\text{TiO}_2$ -imp > Pt/ $\text{TiO}_2$ -pd > Pt/ $\text{TiO}_2$ -cr. These results confirmed that the accessible surface area of the Pt NPs followed in the order Pt/ $\text{TiO}_2$ -imp > Pt/ $\text{TiO}_2$ -pd > Pt/ $\text{TiO}_2$ -cr. X-ray fluorescence revealed that there was no significant difference in Pt content among the three photocatalysts (1.7–1.8 wt%). Therefore, the three Pt-loaded  $\text{TiO}_2$  photocatalysts with almost the same amount of Pt NPs and with different particle sizes were obtained.

Photocatalytic conversions of NO into  $\text{N}_2\text{O}$  over Pt-loaded  $\text{TiO}_2$  photocatalysts were investigated using a quartz fixed-

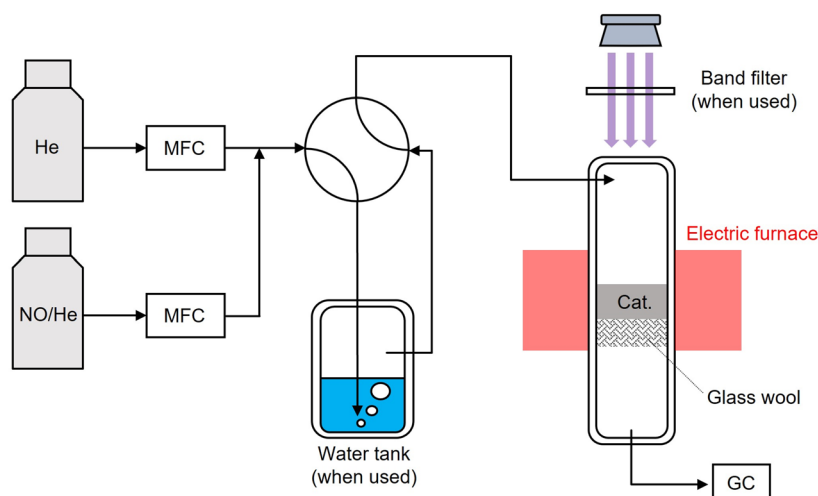


Fig. 2 Schematic of the fixed-bed reactor made in house.



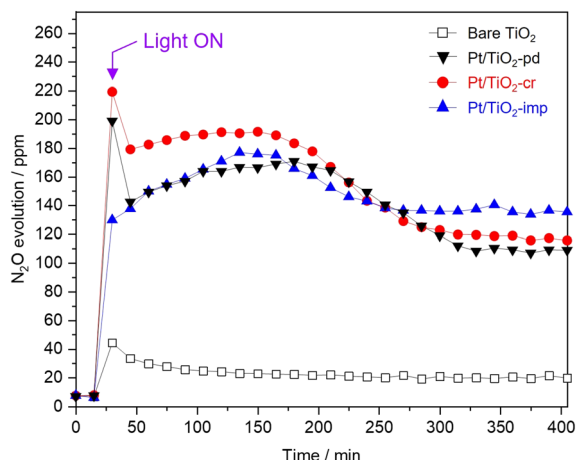


Fig. 3  $\text{N}_2\text{O}$  evolutions over different photocatalysts. Photocatalytic tests were carried out at an SV of  $3500 \text{ h}^{-1}$ .

bed reactor made in house (Fig. 2). Typically, the input gas was passed through the water tank, and UV light was irradiated onto the upper side of the photocatalysts. Prior to photocatalytic tests, samples were pre-treated to completely rid them of carbon species. The details for the photocatalytic tests are described in ESI.†  $\text{N}_2\text{O}$  evolutions over different photocatalysts were compared in Fig. 3. None of the photocatalysts without UV irradiation produced any considerable amount of  $\text{N}_2\text{O}$ . Upon UV irradiation, the evolved amount of  $\text{N}_2\text{O}$  over bare  $\text{TiO}_2$  increased to some extent, and considerably more so did ( $>100 \text{ ppm}$ ) over each of the three Pt-loaded  $\text{TiO}_2$  photocatalysts. These results were indicative of  $\text{N}_2\text{O}$  evolution having been accelerated by light irradiation and of Pt NPs playing a key role in enhancing  $\text{N}_2\text{O}$  evolution. Reaction mechanism is hereafter discussed using Pt/ $\text{TiO}_2$ -pd as the photocatalyst.

Fig. 4 shows representative gas chromatography (GC) profiles of the outlet gases in the photocatalytic tests under UV irradiation. No considerable peak was observed under He flow (in the absence of NO). When NO/He was introduced as

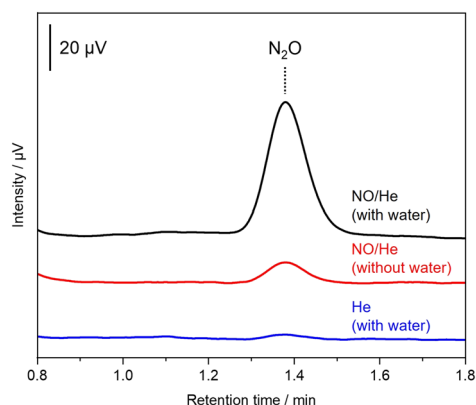


Fig. 4 GC profiles of the gases produced from different feed stocks. The catalytic tests were carried out using Pt/ $\text{TiO}_2$ -pd under UV irradiation at an SV of  $3500 \text{ h}^{-1}$ .

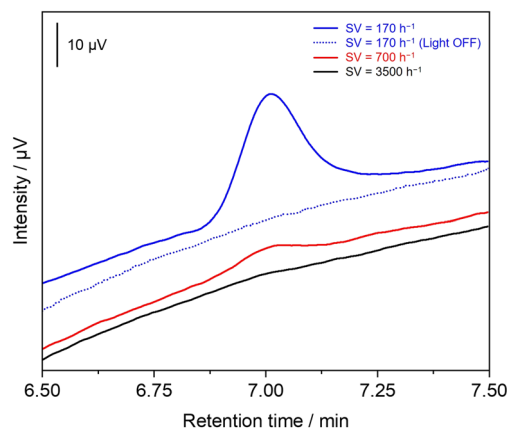


Fig. 5 GC profiles of the product gas over Pt/ $\text{TiO}_2$ -pd under UV irradiation at different SV conditions.

the feedstock gas, there was a peak at 1.36 min, which could be assigned to  $\text{N}_2\text{O}$ . This result indicated that  $\text{N}_2\text{O}$  evolved from the introduced NO. A decreased  $\text{N}_2\text{O}$  evolution was observed when water was not introduced into the reaction system, suggestive of water also playing a part in the photocatalytic reaction.

Fig. 5 shows GC profiles in the region of 6.5–7.5 min at various gas hourly space velocity (GHSV) values. No peak was observed at 7 min for a GHSV of  $3500 \text{ h}^{-1}$  (black line), but peaks at 7 min became obvious at lower GHSV values (red and blue lines). These peaks can be assigned to  $\text{O}_2$ . Furthermore, the peaks originating from  $\text{O}_2$  evolution were not observed at 7 min without UV irradiation (dashed, blue line). In summary,  $\text{O}_2$  evolution was found to be triggered by UV irradiation together with  $\text{N}_2\text{O}$  evolution from NO feed stock. Fig. 6 shows a schematic illustration explaining the proposed mechanism for photocatalytic evolution of  $\text{N}_2\text{O}$  over  $\text{TiO}_2$  with Pt loading. The reductive/oxidative and overall reactions of this system were estimated, and each potential *versus* a normal hydrogen electrode (NHE) can be presented as follows.

Reductive reaction:

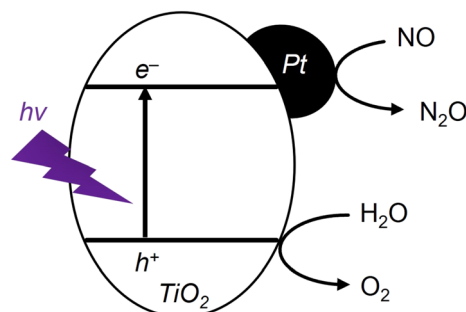
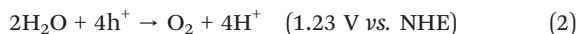


Fig. 6 Proposed mechanism for  $\text{N}_2\text{O}$  evolution over Pt-loaded  $\text{TiO}_2$  under UV irradiation.



Oxidative reaction:



Overall reaction:



Considering the band positions of  $\text{TiO}_2$  (conduction band:  $-0.38 \text{ V vs. NHE}$ , valence band:  $2.82 \text{ V vs. NHE}$ ),<sup>21,22</sup> this photocatalytic reaction (eqn (1) and (2)) would be expected to be able to proceed. Furthermore, consideration of the calculated equilibrium conversion rate (Fig. S3†) suggested the overall reaction (eqn (3)) to be thermodynamically accessible. As for  $\text{O}_2$  in this reaction, inspection of the stoichiometry of eqn (3) would suggest an evolution of half as much  $\text{O}_2$  as  $\text{N}_2\text{O}$  by molarity, but the measured amount of evolved  $\text{O}_2$  was considerably lower (Fig. S4†). Nitrogen dioxide ( $\text{NO}_2$ ) was detected in the outlet gas by using a Fourier transform infrared detector, suggesting that some of the  $\text{O}_2$  reacted with unreacted  $\text{NO}$  to form ( $\text{NO}_2$ ) as shown in eqn (4).



As shown in Fig. 3, Pt loading was observed to enhance the photocatalytic evolution of  $\text{N}_2\text{O}$ , attributed to efficient separation of photogenerated charges. The apparent quantum yield (AQY) was calculated to be 4.4%. This value was comparably higher in gas-phase photocatalysis. Previous research showed the hygroscopic nature of the metal oxide having dramatically increased the AQY of photocatalytic water splitting.<sup>23,24</sup> In the currently investigated  $\text{N}_2\text{O}$  evolution reaction, Pt-loaded  $\text{TiO}_2$  seemed to be quite hygroscopic, resulting in high AQY.

In summary, low-cost  $\text{N}_2\text{O}$  manufacturing approach using  $\text{NO}$  as feed was proposed. The photocatalysts tested hardly converted  $\text{NO}$  into  $\text{N}_2\text{O}$  without UV irradiation, and the amount of  $\text{N}_2\text{O}$  that evolved increased under UV irradiation. In particular, the Pt-loaded  $\text{TiO}_2$  photocatalyst exhibited higher  $\text{N}_2\text{O}$  evolution than did the bare  $\text{TiO}_2$  photocatalyst, suggesting that Pt enhanced the efficiency of photogenerated charges. Furthermore, decreased evolution of  $\text{N}_2\text{O}$  was observed without  $\text{H}_2\text{O}$ , indicative of the involvement of  $\text{H}_2\text{O}$  in this photocatalytic reaction. To the best of our knowledge, this was the first study to demonstrate the photocatalytic evolution of  $\text{N}_2\text{O}$  from  $\text{NO}$ . Although further improvements (e.g., suppression of oxidation of  $\text{NO}$  and increase of conversion rate) is still required, these findings should be considered to help promote the development of  $\text{N}_2\text{O}$  production from a low-cost feedstock.

## Data availability

The data that support the findings of this study are openly available.

## Conflicts of interest

There are no conflicts to declare.

## Acknowledgements

This work was partly supported by the New Energy and Industrial Technology Development Organization (NEDO) under the Moonshot Project, the Japan Society for the Promotion of Science (JSPS), a KAKENHI Grant-in-Aid for Transformative Research Areas (A) JP20A206/20H05880, a Grant-in-Aid for Scientific Research (S) JP23H05454, a Grant-in-Aid for Early-Career Scientists JP24K17585 and the Materials Processing Science project ("Materealize") of MEXT, Grant Number JPMXP0219192801.

## References

- 1 V. N. Parmon, G. I. Panov, A. Uriarte and A. S. Noskov, *Catal. Today*, 2005, **100**, 115–131.
- 2 K. Severin, *Chem. Soc. Rev.*, 2015, **44**, 6375–6386.
- 3 P. Xiao, Y. Wang, Y. Lu, T. De Baerdemaeker, A.-N. Parvulescu, U. Müller, D. De Vos, X. Meng, F.-S. Xiao, W. Zhang, B. Marler, U. Kolb, H. Gies and T. Yokoi, *Appl. Catal., B*, 2023, **325**, 122395.
- 4 P. Xiao, Y. Wang, K. Nakamura, Y. Lu, T. De Baerdemaeker, A.-N. Parvulescu, U. Müller, D. De Vos, X. Meng, F.-S. Xiao, W. Zhang, B. Marler, U. Kolb, R. Osuga, M. Nishibori, H. Gies and T. Yokoi, *ACS Catal.*, 2023, **13**, 11057–11068.
- 5 A. C. Huizink, *Curr. Opin. Psychol.*, 2022, **45**, 101312.
- 6 M. A. Gillman, *Curr. Drug Res. Rev.*, 2019, **11**, 12–20.
- 7 Z. Tang, I. Surin, A. Rasmussen, F. Krumeich, E. V. Kondratenko, V. A. Kondratenko and J. Perez-Ramirez, *Angew. Chem., Int. Ed.*, 2022, **61**, e202200772.
- 8 D. R. MacFarlane, P. V. Cherepanov, J. Choi, B. H. R. Suryanto, R. Y. Hodgetts, J. M. Bakker, F. M. Ferrero Vallana and A. N. Simonov, *Joule*, 2020, **4**, 1186–1205.
- 9 C. D. Dorich, R. T. Conant, F. Albanito, K. Butterbach-Bahl, P. Grace, C. Scheer, V. O. Snow, I. Vogeler and T. J. van der Weerden, *Curr. Opin. Environ. Sustain.*, 2020, **47**, 13–20.
- 10 K. Yamashita, Z. Liu, K. Iyoki, C. T. Chen, S. Miyagi, Y. Yanaba, Y. Yamauchi, T. Okubo and T. Wakiyara, *Chem. Commun.*, 2021, **57**, 1312–1315.
- 11 S. Yamaguchi, P. Hu, H. Ya, P. Xiao, A. Nakata, T. Miyazaki, Y. Morikawa, J. N. Kondo, K. Tange, K. Tonokura, M. Takemoto, Y. Yonezawa, T. Yokoi, K. Iyoki, T. Okubo and T. Wakiyara, *Microporous Mesoporous Mater.*, 2025, **388**, 113550.
- 12 M. Jablonska, *RSC Adv.*, 2022, **12**, 25240–25261.
- 13 S. Mohan, P. Dinesha and S. Kumar, *Chem. Eng. J.*, 2020, **384**, 123253–123262.
- 14 H. Li, X. Yi, J. Miao, Y. Chen, J. Chen and J. Wang, *Catalysts*, 2021, **11**, 906–920.
- 15 Y. Inomata, S. Hata, M. Mino, E. Kiyonaga, K. Morita, K. Hikino, K. Yoshida, H. Kubota, T. Toyao, K.-i. Shimizu, M. Haruta and T. Murayama, *ACS Catal.*, 2019, **9**, 9327–9331.
- 16 B. Suzumura, K. Tanaka, K. Kitazume, S. Hioki, A. Kubo and M. Iwamoto, *Catal. Sci. Technol.*, 2023, **13**, 4131.





- 17 K. Tanaka, B. Suzumura, K. Kitazume, H. Suzuki, H. Teduka and M. Iwamoto, *Catal. Lett.*, 2024, **154**, 2090.
- 18 J. Long, S. Chen, Y. Zhang, C. Guo, X. Fu, D. Deng and J. Xiao, *Angew. Chem., Int. Ed.*, 2020, **59**, 9711–9718.
- 19 A. G. Ramu, R. Renukadevi, P. Silambarasan, I.-S. Moon, M. Govindarasu and D. Choi, *J. Environ. Chem. Eng.*, 2023, **11**, 110751.
- 20 D. Wang, Z. W. Chen, K. Gu, C. Chen, Y. Liu, X. Wei, C. V. Singh and S. Wang, *J. Am. Chem. Soc.*, 2023, **145**, 6899.
- 21 S. B. Rawal, S. Bera and W. I. Lee, *Catal. Lett.*, 2012, **142**, 1482–1488.
- 22 M. Grätzel, *Nature*, 2001, **414**, 338–344.
- 23 T. Suguro, F. Kishimoto, N. Kariya, T. Fukui, M. Nakabayashi, N. Shibata, T. Takata, K. Domen and K. Takanabe, *Nat. Commun.*, 2022, **13**, 5698.
- 24 T. Suguro, F. Kishimoto and K. Takanabe, *Energy Fuels*, 2022, **36**, 8978–8994.

